Optical circulators in two-dimensional magneto-optical photonic crystals

Zheng Wang and Shanhui Fan

Ginzton Laboratory, Stanford University, Stanford, California 94305-4090

We propose an optical circulator formed of a magneto-optical cavity in a 2D photonic crystal. With spatially engineered magnetic domain structures, the cavity can be designed to support a pair of counterrotating states at different frequencies. By coupling the cavity to three waveguides, and by proper matching of the frequency split of the cavity modes with the coupling strength between the cavity and the waveguide, ideal three-port circulators with complete isolation and transmission can be created. We present a guideline for domain design needed to maximize the modal coupling and the operational bandwidth for any given magneto-optical constant. © 2005 Optical Society of America

OCIS codes: 130.3120, 230.3810, 230.5750.

There is a strong interest in the miniaturization of nonreciprocal optical devices and their on-chip integration.[1–7] Such devices suppress multiple reflections between components and thereby improve tolerance with respect to fabrication imperfections and environmental fluctuations. Here we present an analysis of nonreciprocal magneto-optical (MO) resonators in 2D photonic crystals to construct compact, broadband, and planar optical circulators.

The proposed device, shown in Fig. 1, consists of three branches of waveguides (ports) evanescently coupled to a resonant cavity at the center. For simplicity, we assume that the structure has 120° rotational symmetry and use a cavity that supports two counterrotating states at different frequencies $\omega_{+(-)}$. When a wave at frequency ω is incident from port 1, the power transmission coefficients at ports 2 and 3 can be derived as[8]

$$T_{1\to2} = \left| \frac{2}{3}\left[\frac{\exp(i4\pi/3)}{1+i(\omega-\omega_+)/\gamma_+} + \frac{\exp(i2\pi/3)}{1+i(\omega-\omega_-)/\gamma_-} \right] \right|^2,$$

$$T_{1\to3} = \left| \frac{2}{3}\left[\frac{\exp(i2\pi/3)}{1+i(\omega-\omega_+)/\gamma_+} + \frac{\exp(i4\pi/3)}{1+i(\omega-\omega_-)/\gamma_-} \right] \right|^2,$$
$$(1)$$

where the decay rate $\gamma_{+(-)}$ is related to the quality factor $Q_{+(-)}$ as $\gamma=\omega_0/2Q$. When the resonant frequencies are chosen to satisfy the conditions

$$\omega_+ = \omega_0 + \gamma_+/\sqrt{3}, \qquad \omega_- = \omega_0 - \gamma_-/\sqrt{3}, \qquad (2)$$

ports 2 and 3 function as the isolated and the output ports, respectively. (The roles of ports 2 and 3 are switched with $\omega_+<\omega_-$.) The bandwidth for 30 dB isolation is determined from Eqs. (1) to be $0.0548|\omega_+ - \omega_-|/\pi$ in the vicinity of the operational frequency ω_0. Also, by rotational symmetry of the structure, we have $T_{2\to1}=T_{3\to2}=T_{1\to3}=1$, and $T_{1\to2}=T_{2\to3}=T_{3\to1}=0$. Thus, transmission at frequency ω_0 is allowed along only the clockwise direction.

To realize the device described above, we consider a 2D photonic crystal with a triangular lattice of air-holes in a gyrotropic material, such as bismuth iron garnet (BIG, Fig. 2). The airholes have a radius of $0.35a$, where a is the lattice constant. At optical frequencies, the property of a gyrotropic material is characterized by a dielectric tensor,

$$\overleftrightarrow{\varepsilon} = \begin{bmatrix} \varepsilon_\perp & i\varepsilon_a & 0 \\ -i\varepsilon_a & \varepsilon_\perp & 0 \\ 0 & 0 & \varepsilon_\parallel \end{bmatrix}, \qquad (3)$$

when magnetization is along the z direction. Here, for simplicity, we ignore the absorption and assume $\varepsilon_\perp$, $\varepsilon_\parallel$, and ε_a to be real.

To describe the property of this structure analytically we use a Hamiltonian approach.[9] In this approach, the eigenstates of a photonic crystal are calculated by solving $\Theta|\psi\rangle=\omega|\psi\rangle$, where

$$\Theta = \begin{bmatrix} 0 & i\overleftrightarrow{\varepsilon}^{-1}\, \nabla \times \\ -i\mu_0^{-1}\, \nabla \times & 0 \end{bmatrix}$$

defines the Hamiltonian, ω is the eigenfrequency and $|\psi\rangle=[\mathbf{E} \quad \mathbf{H}]^T$ represents the corresponding eigenmode. For the MO photonic crystals, since typically the MO parameter $Q_M=\varepsilon_a/\varepsilon_\perp \ll 1$, we can split $\Theta = \Theta_0+\mathbf{V}$, where
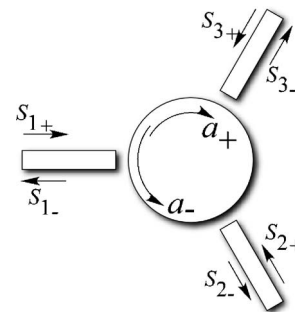

Fig. 1. Schematic of a three-port Y-junction circulator. The straight arrows indicate the incoming and outgoing waves. The curved arrows represent the two counterrotating modes in the resonator.
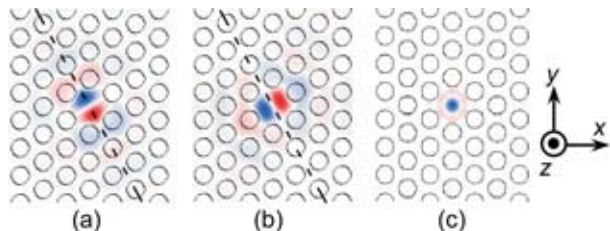
Fig. 2. Blue and red, large positive and negative values, respectively. (a) and (b) Hz fields for the two doubly degenerate cavity modes in a point defect formed by a missing airhole in a photonic crystal. The crystal consists of a triangular lattice of airholes with a radius of $0.35a$, introduced into a dielectric of $\varepsilon = 6.25$. A mirror plane of the crystal is marked with a dashed line in each panel. (c) Spatial distribution of the cross product between the E fields of the two modes shown in (a) and (b).

$$\Theta_0 = \begin{bmatrix} 0 & i\varepsilon_\perp^{-1}\boldsymbol{\nabla}\times \\ -u\mu_0^{-1}\boldsymbol{\nabla}\times & 0 \end{bmatrix},$$

$$\mathbf{V} = \begin{bmatrix} 0 & i(\overleftrightarrow{\varepsilon}^{-1} - \mathbf{I}\varepsilon_\perp^{-1})\boldsymbol{\nabla}\times \\ 0 & 0 \end{bmatrix}. \qquad (4)$$

The unperturbed Hamiltonian Θ_0 entirely describes a nonmagnetic photonic crystal with a scalar dielectric function $\varepsilon_\perp(\mathbf{r})$. The effects of gyrotropy can then be treated by considering $\mathbf{V}$ as a perturbation.

For the structure shown in Fig. 2, the corresponding nonmagnetic photonic crystal described by Θ_0, with $\varepsilon_\perp = 6.25$ as is appropriate for BIG, exhibits a large TE bandgap in the frequency range of 0.302 to 0.403 c/a. Filling a single airhole creates a resonator that supports doubly degenerate dipole modes at a frequency of 0.346 c/a. These two modes can be categorized as an even mode $|e\rangle$ [Fig. 2(a)] and an odd mode $|o\rangle$ [Fig. 2(b)] with respect to a mirror symmetry plane of the crystal. Alternatively, the two eigenmodes can be chosen to be a pair of rotating states $|e\rangle \pm i|o\rangle$.[10] Since Θ_0 by itself possesses time-reversal symmetry, these two rotating modes, which transform into each other with a time-reversal operation, necessarily have the same frequency. To satisfy the condition [Eq. (2)] required to create a circulator, it is therefore essential to use MO materials in the cavity region to break the degeneracy while maintaining the rotating profile.

The effect of the MO material, as described by the operator $\mathbf{V}$, is to introduce MO coupling between the eigenmodes of Θ_0. To the first order of ε_a, the coupling strength between any two modes α and β can be derived as[8]

$$\mathbf{V}_{\alpha\beta} = \frac{i}{2}\sqrt{\omega_\alpha \omega_\beta}\int \varepsilon_a \hat{\mathbf{z}}\cdot(\mathbf{E}_\alpha^* \times \mathbf{E}_\beta)\mathrm{d}V, \qquad (5)$$

where the sign of ε_a is determined by the direction of the magnetization vector. Since states $|e\rangle$ and $|o\rangle$ are both standing-wave modes with real-valued electromagnetic fields, the coupling constant between them is purely imaginary. In the subspace of $|e\rangle$ and $|o\rangle$,

where $\omega_e = \omega_o$, the Hamiltonian of the system is now

$$\begin{pmatrix} \omega_e & \mathbf{V}_{eo} \\ -\mathbf{V}_{eo} & \omega_e \end{pmatrix}$$

in the presence of MO materials. The eigenstates thus become $|e\rangle \pm i|o\rangle$, with frequency splitting of $2|\mathbf{V}_{eo}|$, satisfying the requirement for constructing a circulator ($|\omega_+ - \omega_-| = 2|\mathbf{V}_{eo}|$). In practice, ω_e might deviate from ω_o due to fabrication-related disorders that break the threefold rotational symmetry. However, as long as $|\mathbf{V}_{eo}| \gg |\omega_e - \omega_o|$, $|e\rangle \pm i|o\rangle$ remain the eigenstates of the system. The presence of strong MO coupling thus mitigates such effects of disorders.

Examining Eq. (5), we note that the strength of MO is strongly influenced by the magnetic domain structures. The cross product $\mathbf{E}_e^* \times \mathbf{E}_o$ changes sign rapidly in the cavity [Fig. 2(c)] and overlaps poorly with a uniform domain. On the other hand, the MO coupling can be maximized by designing the domain structures according to the signs of the modal cross product, as shown in the inset of Fig. 3. Alternatively, strong coupling can also be achieved by using a single-domain covering only the center area of the cavity where the modal cross product does not change sign.

A three-port Y-junction circulator can be created by coupling three waveguides to the cavity (Fig. 3, inset). Each waveguide is constructed by enlarging the radius of a row of airholes to $0.55a$. The transport properties of such structures are simulated from first principles by use of a finite-difference time-domain (FDTD) implementation.[11] Here we choose $\varepsilon_a = 0.02463$. The two rotating modes have frequencies 0.3465 (c/a) and 0.3471 (c/a) and quality factors 364 and 367, respectively, satisfying the conditions in Eqs. (2). The FDTD calculations indeed demonstrate nearly ideal three-port circulator characteristics and
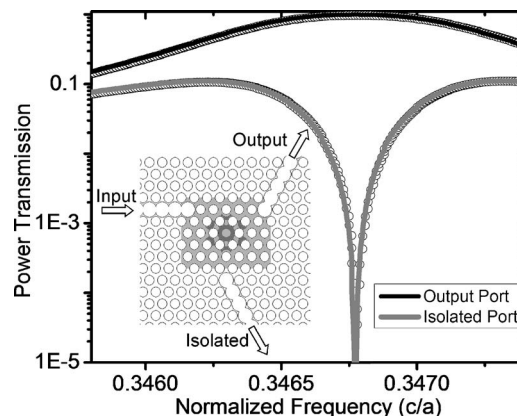

Fig. 3. Inset, transmission spectra at the output and isolated ports of a three-port junction circulator. The circulator is constructed as a point defect coupled to three waveguides. Circles, airholes in BIG. The light and dark gray areas represent the magnetic domains with opposite out-of-plane magnetization directions. The FDTD spectra (circles) agree well with the coupled-mode theory analysis (solid curves).
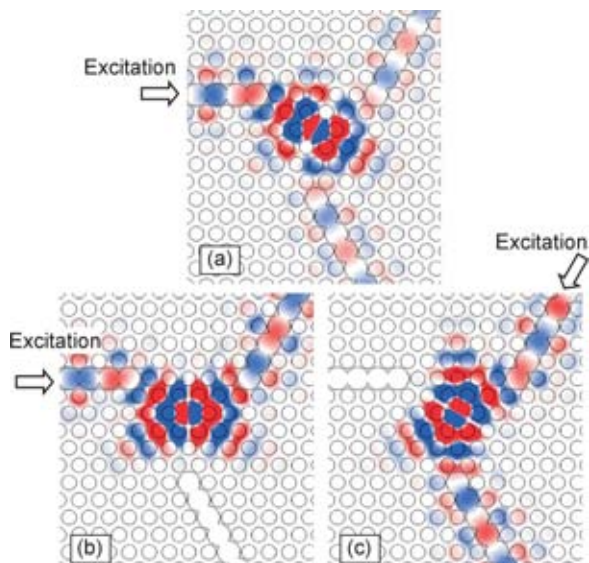
Fig. 4. Out-of-plane H field patterns of the three-port junction circulator shown in Fig. 3 when excited at ω = 0.3468 (c/a). Red and blue represent large positive and negative values, respectively. (a) Non-MO cavity $(\varepsilon_i = 0)$ excited at the input port; (b) MO cavity with $\varepsilon_a = 0.02463$, excited at the input port; (c) MO cavity excited at the output port.

agree nicely with coupled-mode theory (Fig. 3). The bandwidth for 30 dB isolation exceeds 6×10^{-5} (c/a).

The steady-state field patterns at the frequency $\omega_0 = 0.3468$ (c/a) are shown in Fig. 4. In the absence of MO material in the cavity, light is transmitted to both output ports [Fig. 4(a)]. In contrast, the MO resonator shows nearly 100% transmission to the output port and zero transmission to the isolated port [Fig. 4(b)]. Moreover, light that is incident into the output port is completely dropped to the isolated port [Fig. 4(c)]. The input port is therefore free from the backreflections from the output port.

The proposed device occupies only a small footprint of a few wavelengths squared. While the simulation in this Letter is 2D, the coupled-mode theory analysis, and hence the principles of the device, applies to 3D cavity systems, such as photonic crystal slabs. For

implementations in BIG thin films, the material exhibits strong gyrotropy with ε_a saturated at 0.06.[12] The BIG device can provide a large bandwidth for 30 dB isolation up to 213 GHz when operating at 633 nm. Since the quality factor of the resonator as a result of waveguide coupling can be as low as 140, the relatively large material absorption in BIG can still be tolerated. At 1550 nm, Ce:yttrium iron garnet has ε_a saturated at 0.009 with very low absorption.[13] For this material system, the bandwidth for 30 dB isolation at 1550 nm is estimated to be 12.6 GHz.

References

1. R. Wolfe, R. A. Lieberman, V. J. Fratello, R. E. Scotti, and N. Kopylov, Appl. Phys. Lett. **56**, 426 (1990).
2. M. Levy, I. Ilic, R. Scarmozzino, R. M. Osgood, Jr., R. Wolfe, C. J. Gutierrez, and G. A. Prinz, IEEE Photon. Technol. Lett. **5**, 198 (1993).
3. M. Levy, IEEE J. Sel. Top. Quantum Electron. **8**, 1300 (2002).
4. M. Inoue, K. Arai, T. Fujii, and M. Abe, J. Appl. Phys. **83**, 6768 (1998).
5. M. J. Steel, M. Levy, and R. M. Osgood, IEEE Photon. Technol. Lett. **12**, 1171 (2000).
6. Y. Ikezawa, K. Nishimura, H. Uchida, and M. Inoue, J. Magn. Magn. Mater. **272/276**, 1690 (2004).
7. S. K. Mondal and B. J. H. Stadler, IEEE Photon. Technol. Lett. **17**, 127 (2005).
8. Z. Wang and S. Fan, "Magneto-optical defects in two-dimensional photonic crystals," Appl. Phys. B (to be published).
9. Y. Xu, Y. Li, R. K. Lee, and A. Yariv, Phys. Rev. E **62**, 7389 (2000).
10. S. Fan, P. R. Villeneuve, J. D. Joannopoulos, and H. A. Haus, Phys. Rev. Lett. **80**, 960 (1998).
11. A. P. Zhao, J. Juntunen, and A. V. Raisanen, IEEE Trans. Microwave Theory Tech. **47**, 1142 (1999).
12. N. Adachi, V. P. Denysenkov, S. I. Khartsev, A. M. Grishin, and T. Okuda, J. Appl. Phys. **88**, 2734 (2000).
13. M. Huang and S. Y. Zhang, Appl. Phys. A **74**, 177 (2002).